Deglaciation-Induced Spatially Variable Sea-level Change: A Simple-Model Case Study for the Greenland and Antarctic Ice Sheets

M. Kuhn[1], W.E. Featherstone[1], O. Makarynskyy[1,3], W. Keller[2]

[1]Western Australian Centre for Geodesy and The Institute of Geoscience Research, Curtin University of Technology, GPO Box U1987, Perth WA 6845, Australia

[2]Geodaetisches Institute, Universitaet Stuttgart, Geschwister-Scholl-Strasse 24/D, D-70174 Stuttgart, Germany

[3]Now at: Asia-Pacific Applied Science Associates, PO Box 7650, Cloisters Square, Perth WA 6850, Australia

Corresponding Author: Michael Kuhn (phone: +61-8-92667603, fax: +61-8-92662703, e-mail: M.Kuhn@curtin.edu.au)

Abstract

Some studies on deglaciation-induced sea-level change provide only a global average change, thus neglecting the fact that sea-level change is spatially variable. This is due mainly to the gravitational and visco-elastic feedback effects of the changing surface mass loads. In order to redress this apparent misconception and raise further awareness, we provide a conceptual example based on a simulated total melt of the Greenland and Antarctic ice sheets. This would give a global average sea-level change of about 64 m. However, due to the changed distribution of gravitating masses, the sea-level change depends on location, with a range of about -27 m to +79 m (i.e., sea-level will even fall in some places). This spatial dependency has several implications in the case of a total melt, such as >10% biases in global average sea-level change estimates based only on tide-gauge records, flooding of almost 10% of current land areas, an increase of the length of day by almost a half a second and a northward move of the centre of mass (geocentre) by about 20 m.

Keywords: ice sheet, simulated melting, sea-level, length of day, mass centre, flooding, conceptual example

1. Introduction

Recent changes over areas where water is in solid form, the cryosphere, are of current interest as an indicator for global climate change. Based on model results from various climate change scenarios, the third assessment report of the Inter Governmental Panel on Climate Change (IPCC) predicted an increase in global average surface temperature as well as rise in sea-level (e.g., Church et al., 2001; Houghton, 2004), which has now been confirmed by the IPCC's fourth assessment report (Solomon et al., 2007) using observations. It is likely that this currently observed and predicted future increase in global average temperature may cause a partial or complete melt of some parts of the cryosphere (e.g., Oppenheimer, 1998; Huybrects and de Wolde, 1999; Chen et al., 2006; Luthcke et al., 2006, Velicogna and Wahr, 2006, Baur et al., in press), which in turn will alter global sea-level (e.g., Gregory and Oerlemans, 1998; Church et al., 2001; Cazenave and Nerem, 2004; Houghton, 2004).

Due to many scientific and socioeconomic reasons, sea-level change is currently a major area of research and public interest, which is also due to the possibility that significant coastal areas can be flooded. Currently, a huge amount (about 3 x 10^7 km^3) of freshwater is locked in the Greenland and Antarctic ice sheets, which is estimated to alter global average sea-level by about 70 m (e.g. Rignot and Thomas, 2002, Alley et al., 2005) when completely melted and uniformly distributed over the oceans (termed here as eustatic change). Rowley et al. (2007), for example, show that only a 6 m global average sea-level rise will affect more than 400 million people, which is about 7% of today's world population. However, like Rowley et al. (2007), the majority of deglaciation-induced sea-level change studies only consider a globally uniform change (e.g., Chao and O'Connor, 1987; Gregory and Oerlemans, 1998; Huybrechts and de Wolde, 1999; Lambeck et al., 2002; Houghton, 2004; Chen et al., 2006 amongst many others). This is unrealistic as changes in the cryosphere will actually result in a non-uniform sea-level change. The spatial dependency is due mostly to the self-gravitation and visco-elastic response of the changing surface mass and load distribution. Even though this behaviour has been known for a long time, with an early reference given by Woodward (1888) and subsequent improved formulations by various authors (e.g. Farrell and Clark, 1976; Mitrovica et al., 2001; Clark et al., 2002), it is neglected in many studies focusing only on the eustatic sea-level change.

In order to redress this possible misconception, we revisit deglaciation-induced sea-level changes and use the total melt of the Greenland and Antarctic ice sheets as an educational example in order to demonstrate the main principles. We confirm that deglaciation-induced sea-level change is not uniform and can differ considerably locally and/or regionally from the eustatic change. Indeed, we show that sea-level can even fall in some regions, notably close to the melting ice masses. While the simplistic view of an eustatic sea-level change is satisfactory when quantifying the global average, we show that the spatial variability is important in the interpretation of past (e.g., Farrell and Clark, 1976; Clark et al., 2002), present (e.g., Conrad and Hager, 1997; Tamisiea et al., 2001) and future (e.g., Mitrovica et al., 2001; Gregory and Huybrechts, 2006, Mitrovica, et al. 2009) sea-level change. We demonstrate that neglecting these effects can lead to considerable biases in global average sea-level estimates from spatially-limited tide gauge and/or satellite altimeter observations, as is commonly done today (e.g. Douglas, 2001; Nerem and Mitchum, 2001; Cazenave and Nerem, 2004). Such spatial biases have been mentioned by e.g. Conrad and Hager (1997) and Tamisiea et al. (2001), but not quantified for a partial or complete melt of the polar ice sheets.

In section 2 of this contribution, we revisit the general theory for deglaciation-induced sea-level change and discuss the primary and secondary effects. In section 3, we provide and discuss our simple-model numerical examples. We first apply the theory described in section 2 to three melting scenarios of the polar ice sheets by considering only the primary effects in order to provide a conceptual example on the spatial variability of deglaciation-induced sea-level change. Furthermore, for the purpose of an educational example, we also provide estimates on changes in the Earth's rotation, centre of mass (geocentre), spatial sea-level bias and land-ocean distribution considering primary effects only.

2. Simulation of Deglaciation-Induced Sea-level Change

In order to provide a conceptual example, we have simulated global sea-level change based on three extreme melting scenarios: (Scenario A) total melt of the Greenland ice sheet and all glaciers in the Northern Hemisphere; (Scenario B) total melt of the Antarctic ice sheet and all glaciers in the Southern Hemisphere, and (Scenario C) complete melt of all grounded ice masses located above current mean sea-level (MSL). These scenarios where chosen for the sole purpose of demonstrating the spatial variability of deglaciation-induced sea-level change, so should **not** be interpreted as likely future sea-level change scenarios. However, while a total melt of the Antarctic ice sheet (especially the East Antarctic ice sheet) over the next few millennia is very unlikely, a partial or total melt of the Greenland ice sheet and considerable loss of West Antarctic ice sheet over a few-century time-scale seems possible under current greenhouse warming conditions (e.g., Huybrechts and de Wolde, 1999; Church et al., 2001; Huybrechts et al., 2004, Ridley et al., 2005, Mitrovica et al., 2009). Furthermore, it is very likely that under current global warming conditions mountain glaciers will decrease rapidly in the 21st century leaving the polar ice sheets as major contributors to sea-level change on a few-century time-scale (e.g., Raper and Braithwaite, 2006). For our simple-model simulation, the information on the volume and spatial distribution of ice-masses, ocean water and land masses is taken from the JGP95E global 5-arc-minute by 5-arc-minute digital elevation model (Lemoine et al., 1998, chapter 2) to define the initial reference state of our simulations.

Our determination of the relative sea-level change, i.e. the sea surface with respect to the visco-elastically deformable Earth's surface (as would be sensed by tide-gauges), is based on Farrell and Clark (1976) for a non-rotating visco-elastic Earth model. Accordingly, the new relative sea-level depends on the amount and spatial distribution of ice melted, changes in the Earth's gravity field due to redistribution of masses, and the visco-elastic response of the Earth's surface. The latter requires information on the rheology of the Earth's interior and temporal evolution of the changing ice masses.

Based on Farrell and Clark (1976), the relative sea-level change can be symbolically expressed as (today often termed as sea-level equation, e.g., Mitrovica and Milne 2003)

$$S_r(\Omega) = S_{eu} + \left(S_{\Delta\Phi}(\Omega) - < S_{\Delta\Phi}(\Omega) >_o\right) - \left(U_{ve}(\Omega) - < U_{ve}(\Omega) >_o\right) \qquad (1)$$

where the spatial dependency is expressed by the coordinate pair Ω = (φ: latitude, λ: longitude) and the integral average over the ocean area is indicated by $< \cdot >_o$. The global average change in sea-level due to the freshwater influx from melted ice masses is given by the eustatic change S_{eu}, thus the water-equivalent that has been adjusted for the mass-density difference between ice and freshwater is uniformly distributed over the total ocean surface.

The second term in eqn. (1) indicates the vertical change of the equipotential surface coinciding with current MSL due to the change in the Earth's gravitational potential $\Delta\Phi(\Omega)$, the perturbing potential with respect to the assumed reference state, including the effects of mass changes due to the visco-elastic response is given by $S_{\Delta\Phi}(\Omega) = \Delta\Phi(\Omega)/g$, where g is the gravitational acceleration at the Earth's surface. Essentially, three single effects on the Earth's gravitational potential are included in $\Delta\Phi(\Omega)$: (1) changes in ice masses, (2) changes in ocean water distribution and (3) visco-elastic changes of the Earth's crust. The term $U_{ve}(\Omega)$ indicates the vertical displacement of the Earth's surface due to the visco-elastic response, which has to be considered when studying relative sea-level change. The global average terms $< S_{\Delta\Phi}(\Omega) >_o$ and $< U_{ve}(\Omega) >_o$ have been subtracted in eqn. (1) so that the total mass change over the oceans is only due to the eustatic sea-level change e.g. $< S_r(\Omega) >_o = S_{eu}$.

Figure 1 provides a cartoon that illustrates the principles of deglaciation-induced sea-level change as obtained by applying eqn. (1) to melting ice masses. The cartoon is similar to that provided by Fig. 6 in Farrell and Clark (1976) but shows clearly the spatial sea-level variability. Panel A of Fig. 1 indicates the present situation where huge ice masses are locked in the polar ice sheets. Following Newton's law of gravitation, the ice masses exert an attraction on the ocean water masses, pulling water towards the ice sheet. Once the ice masses have been partly or completely melted (Panel B of Fig. 1), the gravitational attraction has been reduced or removed, therefore releasing previously attracted ocean water. This means that, apart from fresh water influx from melting ice masses, there will be a change in global ocean water mass distribution due to mostly the gravitational feedback effect, which also includes gravitational effects due to the visco-elastic change of the Earth's crust. As indicated in Panel B of Fig. 1, this effect leads to a smaller than the eustatic sea-level rise (including fall) close to the melting ice masses and a larger rise at more distant locations. In addition to the gravitational effects Panel B of Fig. 1 also indicates a vertical change of the Earth's surface due to the visco-elastic effect, which is important to consider when studying relative sea-level change as would be observed by a tide gauge located on the deforming Earth's surface. The visco-elastic effect generally manifest as a relaxation (uplift) over the area of ice melt and a loading (depression) over the ocean areas.

[Figure 1 near here]

As this study only aims to demonstrate the general principles, we do not include any viscous effects as well as other secondary effects in our simulations, therefore dealing only with the gravitational and elastic feedbacks $S_{\Delta\Phi}(\Omega)$ and $U_e(\Omega) = U_{ve}(\Omega)$, respectively. In particular, we neglect viscous effects due to current and future ice melt as well as from past glacial cycles, feedback effects from a change in Earth rotation and land-ocean distribution and thermal expansion of ocean water due to warming. The secondary effects have been neglected because they are at least one order of magnitude smaller than the primary signal

$S_r(\Omega)$ for a total melt scenario, therefore do not change the conceptual example and general conclusions made here. However, it has to be stated clearly that numerical results may differ from our results when properly including all secondary feedback effects. The interested reader is referred to, e.g., Nakiboglu and Lambeck (1991), Milne and Mitrovica (1998), Milne et al. (1999), Peltier (2001), Mitrovica and Milne (2003), Lambeck (2003), Mitrovica et al. (2005), Mitrovica et al. (2009) and the literature review in Mitrovica (2003), which all provide more sophisticated modelling techniques including various secondary effects. For completeness, an additional term should be added on the right-hand side of eq. (1), which accounts for all second-order effects that have been neglected here. Again, we only aim to highlight the gravitational feedback effect, as opposed to claiming a model that is completely realistic.

Long-term effects of glacial isostatic adjustment (GIA) induced from past, current and future surface load changes are neglected, as their magnitudes are mostly <1 m (e.g., Nakiboglu and Lambeck, 1991, Peltier, 2001) under the assumption that the complete melt takes place over a few thousand years, hence elastic feedback is dominant. Close to the melting ice masses, however, the effect can get more pronounced. Thermal expansion can contribute several meters to sea-level change over a few thousand years (e.g., Makarynskyy et al., 2007). While being an important contributor to current and near-future sea-level change (e.g. Solomon et al., 2007), steric sea-level changes are of minor importance when considering long-term deglaciation scenarios with the major contribution to sea-level change coming from the Polar ice sheets. In addition, steric sea-level changes have practically no influence on the Earth’s gravity field (e.g. Roedelsperger et al., 2008). Under a total melt scenario, the change in land-ocean distribution has also a feedback effect on global average sea-level by several metres as will be demonstrated below, thus can also be considered as secondary effect. In relation to the magnitudes provided above, feedback effects from changes in the Earth's rotation are considerably smaller (e.g., Milne and Mitrovica, 1998).

As both the gravitational and elastic feedback effects are linearly related to the change in the Earth's gravitational potential $\Delta\Phi(\Omega)$, deglaciation-induced sea-level change (cf. eqn. 1) can be modelled by the application of forward gravity modelling techniques only, thus requiring an integration over space but not over time. This, however, requires the information of an elastic Earth model in which the elastic change of the Earth's crust is linearly related to $\Delta\Phi(\Omega)$ via the corresponding elastic load Love numbers. Here we base our simple-model numerical simulations on the load Love numbers derived in Farrell (1972) for the Gutenberg-Bullen model A. To calculate the effects on the gravitational potential, we apply Newton's integral expressed by a spherical harmonic expansion (e.g., Ramillen, 2002), implicitly approximating all mass changes by surface mass changes (e.g., Kuhn and Seitz, 2005). Furthermore, we assume that all melt-water is transferred into the oceans, neglecting changes in land hydrology and the atmosphere. While climate change scenarios show considerable changes in the global hydrological cycle, they are still uncertain in terms of the magnitude and spatial distribution (e.g., Church et al., 2001; Oki and Kanae, 2006), thus their effect on sea-level is difficult to assess, hence the need for this assumption/simplification.

As the determination of both $\Delta\Phi(\Omega)$ and $U_e(\Omega)$ require the knowledge of the relative sea-level change $S_r(\Omega)$ (redistribution of all surface masses), the computation is iterative with the first iteration given by the eustatic change. However, the iteration procedure converges very quickly and the results here are based on four iterations, resulting in maximum relative errors of 0.1 %.

3. Results

3.1. Global Sea-level Change

In order to provide estimates on deglaciation-induced sea-level change, we use the amount and spatial distribution of the ice-masses contained in JGP95E (Lemoine et al., 1998, chapter 2), which will be scrutinised first. The calculation of their eustatic sea-level equivalent, when uniformly distributed over the oceans (with a total surface of 3.62 x 10^8 km^2), is based on a sphere of radius 6,378,137 m and mean mass-densities of ice and fresh water of 927 kg m^{-3} and 1000 kg m^{-3}, respectively. Table 1 shows the global ice volume and that contained in the ice sheets of Greenland and Antarctica and the estimates of the corresponding eustatic sea-level change should they melt completely. Most of the ice masses are concentrated over Antarctica (~90%) and Greenland (~9%) with only a minor quantity contained in the global glaciers (<1%).

We only consider ice masses located above current MSL, thus neglecting the isostatic uplift of ice masses during the melting period. The corresponding relative effect on sea-level is <<1% as the amount of vertical uplift of the Earth's crust is <1% compared to the thickness of the melted ice masses. Ice masses below current MSL may only become floating ice with respect to ocean water, thus only having a secondary effect on global average sea-level change, which is due to the mass-density difference between ice and ocean water with the latter density taken here as 1028 kg m^{-3}. This effect is only about 1% (70 cm) of the total average sea-level change in the case all ice masses below the current sea-level are melted (see Table 1).

[Table 1 near here]

The estimates in Table 1 are considerably smaller than the widely cited global average sea-level rise of about 80 m for a total melt of all ice (e.g., Williams and Ferrigno, 1999). The difference is partly based on the information given by a glaciological and geophysical folio of Antarctica (Drewry, 1983). The corresponding value of 73 m for the Antarctic ice sheet includes all ice masses below current MSL, as well as erroneous topographic data (e.g., Huybrechts et al., 2000, Lythe et al., 2001). More recent estimates show a value of about 57 m for the contribution of the Antarctic ice sheet only including ice masses above current MSL (e.g., Huybrechts et al., 2000), which matches the estimate presented in Table 1. As such, we believe the use of JGP95E gives a reliable estimate of the ice-mass distribution over the poles. Also, recall that this is a simple model simulation to highlight that self-gravitational and elastic feedback causes sea-level change to be spatially variable.

Considering the self-gravitational and elastic feedback effects for the three melting scenarios described in section 2, Figures 2 to 4 show that the resulting sea-level change is definitely not uniform, with the eustatic sea-level change present only along one particular isoline close to the equator, but not coincident with it. Due to self-gravitation, regions in close proximity to the melted ice masses show a smaller sea-level change and, correspondingly, more distant regions show a larger change compared to the eustatic one, even with sea-level fall very close to the melting ice masses.

[Figures 2 to 4 near here]

Assuming a complete melt of the Greenland ice sheet only, while Antarctica remains stable (e.g., Huybrechts and de Wolde, 1999; Huybrechts et al., 2004, Ridley et al., 2005), sea-level over most locations in the Northern Hemisphere shows a considerably smaller rise the eustatic one, whereas it is larger in the Southern Hemisphere (Figure 2). In large regions around Greenland, reaching as far as the coast of Newfoundland, the entrance of Hudson Bay and almost the coast of Scandinavia, sea-level will fall, instead of rise. The situation is reversed if only the Antarctic ice sheet is melted (Figure 3). Sea-level rise is generally higher than the eustatic level in the Northern Hemisphere and smaller in the Southern Hemisphere. Due to the much larger ice volumes involved, only a few places very close to the Antarctic coast will experience sea-level fall. As most ice masses are currently located over Antarctica (~ 90%), the spatial sea-level change pattern for a complete melt is dominated by this second scenario (compare Figure 4 with 3).

While Figures 2 to 4 show sea-level after a complete melt of all ice masses the situation for a partial melt can be approximately obtained by scaling the results of the complete melt scenarios. This property was already discussed by Farrell and Clark (1976), leading to the common use of a normalised sea-level change pattern where actual sea-level is divided by the eustatic equivalent. When normalising the results of Figures 2 to 4, the resulting spatial patterns are very similar, but not identical, to that presented in Conrad and Hager (1997) and Mitrovica et al. (2001), which are based on present-day melting of ice sheets and glaciers, whereas our results are based on simulated (future) melting. The visual similarity demonstrates that absolute sea-level change is almost linearly related to the amount of ice melted, thus scaling of the results obtained for the total melt scenario is generally permitted to gain the result for a partial melt scenario.

However, examining the structure of Newton's integral, there is only an exact linear relationship if the relative amount of the melting ice masses is changed but the geometry remains unchanged, which means a change in ice masses is only quantified by a density change. In other words, a thin ice sheet has to melt by exactly the same relative amount than a thick ice sheet. This behaviour, however, is rather unlikely, as under the same warming conditions, thin ice sheets should normally disintegrate first before thick ones. Considering this behaviour, we estimated that a 1% melt scenario scaled to a total melt scenario (e.g., extreme case of scaling) can lead to relative errors in excess of 20% in the final sea-level close to the melting ice masses. However, further away from the melting ice masses, the relative error diminishes rather quickly with distance.

3.2. Changes in the Earth's Rotation and Centre of Mass

In order to show some other implications of deglaciation-induced sea-level changes on the system Earth, we provide information on changes in the Earth's rotation rate and centre of mass, both directly related to changes of the Earth's mass distribution. Like for the spatial sea-level change pattern provided in the previous section, it should be mentioned here that the numerical values provided serve only to illustrate the general effects and more sophisticated modelling by including other (secondary) effects will lead to different numerical results but the same broad conclusions.

The spatially variable sea-level change pattern in Figures 2 to 4 imply a general mass transport from Polar Regions towards the equator, resulting in the Earth's gravitational oblateness to increase, rotation rate to decrease, and the centre of mass to change (Table 2). These changes have been derived for our three melting scenarios using (fully normalised and unit less) Stokes's coefficients ΔC_{nm}, ΔS_{nm} (*n*: degree, *m*: order) associated to the change in gravitational potential corresponding to the different surface mass transports. The changes in J_2 (gravitational oblateness or dynamical form factor) and length of day (LOD) are based on the degree-two zonal harmonic coefficient C_{20} following the relation given in Chao and O'Connor (1987):

$$\Delta J_2 = -\sqrt{5}\Delta C_{20} \tag{2}$$

$$\Delta LOD = \frac{2MR^2}{3C} LOD\, \Delta J_2 \tag{3}$$

with M and R being the Earth's mass and mean radius, respectively and C is the Earth's polar moment of inertia. Equation (3) holds for a net mass change of zero, thus all ice masses are transferred into the oceans. Heiskanen and Moritz (1967) show that changes in the Earth's centre of mass expressed by the three dimensional Cartesian coordinate differences ΔX , ΔY and ΔZ are directly related the degree one Stokes coefficients through the relation

$$\begin{Bmatrix} \Delta X \\ \Delta Y \\ \Delta Z \end{Bmatrix} = \sqrt{3}R \begin{Bmatrix} C_{11} \\ S_{11} \\ C_{10} \end{Bmatrix}. \tag{4}$$

[Table 2 near here]

As the bulk of the land-based ice masses are concentrated in the polar ice sheets, any melting will result in a slowdown of the Earth's rotation, thus an increase in LOD. The complete melt of the Greenland ice sheet (scenario A) already results in a LOD increase of 40 milliseconds while the increase is 0.41 sec and almost a half a second for a complete melt of the Antarctic ice sheet (scenario B) and a complete melt of all land based ice masses (scenario C), respectively (see Table 2). A change in the Earth's centre of mass always points away from the removed masses, the polar ice sheets. Therefore, a complete melt of the Greenland ice sheet (scenario A) results mostly in a southwards movement of the Earth's centre of mass by >3 metres. The opposite happens for a complete melt of the Antarctic ice sheet (scenario B) resulting in a mostly northwards shift of >21 metres. The total melt of all land based ice masses (scenario C) once again is dominated by scenario B as most of the ice mass is concentrated over the Antarctic ice sheet.

Both the change in the Earth's rotation and centre of mass are several orders of magnitude greater then currently observed short-term (e.g. seasonal) and long-term (e.g. century-scale) changes. Observed LOD changes are in the order of milliseconds both seasonal and secular over a century-scale (e.g., Gross 2008), thus about two to three orders of magnitude smaller than that of the three melting scenarios presented. For the Earth's centre of mass, the observed changes are three to four orders of magnitudes smaller, being in the range of millimetres to about one centimetre (e.g. Dong et al. 1997). Therefore, it can be expected that these changes will have major impacts on the precise definition of terrestrial reference frames in particular (e.g., Dong et al. 2003) and the dynamic system Earth in general.

3.3. Spatial Sea-level Biases

The consequence of the spatially variable sea-level change patterns in Figures 2 to 4 becomes important when trying to derive global average sea-level change estimates (e.g., Conrad and Hager, 1997; Tamisiea et al., 2001, Cazenave and Nerem 2004) from either poorly distributed tide-gauge observations or satellite radar altimeter measurements that currently omit polar regions due to the satellites' orbital inclination.

This spatial sampling effect is sometimes neglected when interpreting the results from tide-gauge records and/or satellite altimeter data (cf. Douglas, 2001; Nerem and Mitchum, 2001). Under the assumption of a specific melting scenario, however, these effects can be quantified by examining Figures 2 to 4. In the extreme case when only one tide-gauge station is used, the bias in the corresponding global sea-level change can be overestimated by about 30% or underestimated by over 100% (i.e., sea-level fall instead of rise) as can be derived by comparing the minimum and maximum sea-level changes with the corresponding eustatic change in Figures 2 to 4. As such, the gravitational feedback effect is a key element in properly interpreting current estimates of global sea-level change. Hagedoorn et al. (2007), for example, use this property to derive an optimal combination between various mantle viscosity models and ice history models by comparison their sea-level response with Holocene relative sea-level records.

Based on the frequently used 27 tide-gauges selected by Douglas (2001), average sea-level rise could be overestimated by > 10% under the melting scenarios considered here (Table 3). Importantly, the bias does not depend on the length or quality of the tide-gauge records, but only on their locations. This situation does not improve when using all the tide-gauge records (almost 2000) provided by the Permanent Service for Mean Sea-level (PSMSL) (Woodworth and Player, 2003) regardless of the tide-gauges' operational status; the biases are also around 10%. These biases result from insufficient sampling of the world's oceans by tide-gauges. Even for satellite altimeter data, the world's oceans are insufficiently sampled because Polar Regions are omitted. However, due to the more uniform coverage of altimetry, the biases are smaller and in the range of a few percent (Table 3).

[Table 3 near here]

One could argue that the biases presented in Table 3 are of minor importance, since they show a similar magnitude to current uncertainties in sea-level change estimates obtained by long-term tide-gauge records or satellite altimeter measurements (e.g., Cazenave and

Nerem, 2004). However, the biases presented are *systematic* and can only be improved by a different sampling of the world's oceans, rather than focussing on improving the data quality. This is where gravitational feedback, which is rather simple to model using Newtonian forward modelling, is of use to simulate a broad-scale picture of the spatial variability of sea-level change, thus reducing the exposure to biasing due to observation-location sampling.

3.4. Change in Land-Ocean Distribution

In case of sea-level rise, coastal areas are naturally subject to flooding, thus the current land-ocean distribution (coastline) will change (e.g., Nicholls, 2002, Pilkey and Cooper, 2004, Rowley et al., 2007). The extent of flooding, however, also depends on the spatial pattern of sea-level rise. As an example, we simulate the flooding of coastal areas based on the spatial sea-level change patterns in Figure 2 to 4 and the elevation data provided by JGP95E (Lemoine et al., 1998, chapter 2). In our flooding simulations, we consider the natural flow of water along equipotential surfaces rather than simply matching the new sea-level with the corresponding elevation isoline on land. This is important as there is a negative feedback effect that lowers the overall sea-level rise as water is spread out over land, thus is distributed over a larger area (e.g., Mitrovica and Milne, 2003). This negative feedback effect can reduce the eustatic sea-level change values given in Table 1 by up to 3%. However, the effect of erosion due to different coastal morphology has not been considered, which can extend or restrict the affected area considerably (e.g., Bruun, 1988, Zhang et al., 2004). Apart from flooding, some land reclamation close to the large ice sheets will also occur.

Table 4 provides for the three flooding simulations considered here (Section 2), some numerical results including the relative change in land and ocean areas, the magnitude of the above mentioned negative feedback effect as well as the amount of present-day world population affected. The latter has been derived by matching the flooded area with gridded population data of the world provided by the Centre for International Earth Science Information Network (GWPFE, 2005). Importantly, the estimates on the world population affected by flooding are purely hypothetical as we assume that a total melt takes place over at least few thousand years and a prediction of the amount and spatial distribution of the world population over such time period is not possible. Therefore, the estimates should be treated more as an indication of the potential vulnerability of current world population due to catastrophic flooding.

Naturally, the most prominent flooding scenario is obtained for a complete melt of all ice masses (Figure 5). Under such scenario, all large river deltas and many low-lying regions such as large parts of the Ganges river basin including most of Bangladesh, many nations in South-East Asia, the West Siberian Plain and North Siberian Lowland, the low-lying countries in Northern Europe and the South-East coast of North America including most of Florida will be flooded. Our flooding scenario also reveals that the Caspian and Aral Seas will be flooded even though they do not have any current connection to the world's oceans. This is because, according to the elevation data in JGP95E, there are low-lying areas through the Don and Volga river valleys that connect the Caspian Sea with the Black Sea and a low-lying passage through Turkmenistan from the South Caspian Sea to the Aral Sea. The existence of such passages has to be verified through local elevation data, and may change the data in Table 4 if these areas are not included in the flooding scenario. However, this region illustrates a good example for the flooding of basin areas that are only reached once the rising sea-level breaches a natural barrier upon which the whole basin (area with lower elevations then the natural barrier) may be flooded.

Under such an extreme and hypothetical scenario, almost one third of the present-day world population will be affected (cf. Table 4) illustrating the fact that large amount of the present-day world population is living either close to the coast or in low-lying areas, thus is vulnerable to sea-level rise. Even a rather modest amount of about 7 m global average sea-level rise (e.g. only the Greenland ice sheet is melted, cf. Table 1) the present day coastline changes considerably, directly affecting about 4.5% of today's world population. This effect is much smaller than the 7% derived by Rowley et al. (2007) for only 6 m global average sea-level rise. As the latter estimate is based on a globally uniform sea-level rise, the difference illustrates the effect when accounting for the spatial variation in global sea-level change (cf. Figures 2 to 4). As most of the world's population is concentrated on the Northern Hemisphere, a lower value of the affected world population should be expected as a complete melt of the Greenland ice sheet will result in a lower then average sea-level rise over large parts of North America and Europe (cf. Figure 2).

[Table 4 near here]

[Figure 5 near here]

4. Summary and Conclusions

We have provided a conceptual example on deglaciation-induced sea-level change based on the total melt of the Greenland and Antarctic ice sheets. We have shown, due to the self-gravitational effects of the changed surface mass distribution due to ice-melt, global sea-level change is spatially non-uniform. This is contrary to many studies that assume only a eustatic sea-level change.

Neglecting the spatial variability of sea-level rise can adversely affect the estimate of global average sea-level change values based on poorly distributed tide-gauge and/or satellite altimetry measurements, leading to relative biases in excess of 10 %. Therefore, this information has to be considered when selecting a set of long-term tide gauge records that will lead to a largely improved or even “bias-free” estimate of global average sea-level change.

Based on past and present observations of global sea-level change, the corresponding sea-level change pattern can provide valuable information to address the so called “attribution problem”, the delineation where a mass change in the cryosphere is currently taking place or has occurred in the past.

Our simple-model results have also shown that spatially varying sea-level change will cause different levels of flooding of coastal areas, as opposed to what would be expected by simplistically applying only a single-value representing a globally uniform sea-level change. This effect has been demonstrated for the spatial sea-level change pattern calculated here where estimates of coastal vulnerability can vary considerably with respect to the use of a globally uniform change. This also holds for estimates of changes in land-water distribution due to mostly flooding of coastal areas.

Finally, we conclude that under the three extreme melting scenarios the presented changes of sea-level, Earth’s rotation and centre of mass will have major impacts on the dynamic system Earth in general and the precise definition of terrestrial reference frames in particular. This is based on the fact that all presented changes are several orders of magnitude larger then currently observed changes.

Acknowledgements

This research is supported by the Australian Research Council through Discovery Project grants DP0345583 and DP0877381. We thank two anonymous reviewers for their valuable comments and critiques that helped to significantly improve the original manuscript. This is TIGeR publication xxx.

References

Alley, R.B., Clark, P.U., Huybrechts, P., Joughin, I., 2005. Ice-Sheet and Sea-Level Changes. Science, 310, 456-460.

Baur, O., Kuhn, M., Featherstone, W.E. 2009. GRACE-derived ice-mass changes over Greenland by accounting for leakage effects. J Geophys Res (submitted).

Bruun, P., 1988. The Bruun rule of erosion by sea-level rise: A discussion on large-scale two- and three-dimensional usages, J. Coastal Res., 4, 627-648.

Cazenave, A., Nerem, R.S., 2004. Present-day sea-level change: observations and causes. Rev. Geophys. 42, RG3001, 1-20.

Chao, B.F., O'Connor, W.P., 1987. Effect of a uniform sea-level change on the Earth's rotation and gravitational filed. Geophys. J. Int. 93, 191-193.

Chen, J.L., Wilson, C.R., Tapley, B.D., 2006. Satellite Gravity Measurements Confirm Accelerated Melting of Greenland Ice Sheet. Science 313, 1958, doi:10.1126/science.1129007.

Church, J., Gregory, J.M., Huybrechts, P., Kuhn, M., Lambeck, K., Nhuan, M.T., Qin, D., Woodworth, P.L., 2001. Changes in Sea-level. In: Houghton, J.T., Ding, Y., Griggs, D.J., Noguer, M., Van der Linden, P.J., Xiaou, D. (Eds.), Climate Change 2001, The Scientific Basis. Contributions of Working Group I to the third Assessment Report of the

Intergovernmental Panel on Climate Change. Cambridge University Press, Cambridge, pp. 639-694.

Clark, P.U., Mitrovica, J.X., Milne, G.A., Tamisiea, M.E., 2002. Sea-level fingerprinting as a direct test for the source of global meltwater pulse 1A. Science 295, 2438-2441.

Conrad, C.P., Hager, B.H., 1997. Spatial variations in the rate of sea-level rise caused by the present-day melting of glaciers and ice sheets. Geophys. Res. Lett. 24, 1503-1506.

Dong, D., Dickey, J.O., Chao, Y., Cheng, M.K., 1997. Geocentre variations caused by atmosphere, ocean and surface ground water. Geophys. Res. Lett., 24(15), 1867-1870.

Dong, D., Yunck, T., Heflin, M. 2003. Origin of the International Terrestrial Reference Frame. J. Geophys. Res., 108(B4), 2200.

Drewry, D. J., 1983. Antarctica: Glaciological and Geophysical Folio, Scott Polar Res. Inst., Cambridge, England, U.K.

Douglas, B.C., 2001. Sea-level Change in the Era of the Recording Tide Gauge. In: Douglas, B.C., Kearney, M.S., Leatherman, S.P. (Eds.), Sea-level Rise, History and Consequences. Academic Press, London, pp. 37-64.

Farrell, W.E., 1972. Deformation of the Earth by Surface Loads. Rev Geophys and Space Physics 10, 761-797.

Farrell, W.E., Clark, J.A., 1976. On postglacial sea-level. Geophys. J. R. astr. Soc. 46, 647-667.

Fu, L.F., Cazenave, A., 2001. Satellite Altimetry and Earth Sciences – A Handbook of Techniques and Applications. International Geophysical Series, Vol. 69, Academic Press, San Diego California.

GPWFE, 2005. Centre for International Earth Science Information Network (CIESIN), Columbia University; United Nations Food and Agriculture Programme (FAO); and

Centro International de Agricultural Tropical (CIAT) 2005. Gridded Population of the World: Future Estimates (GPWFE). Palisades, NY: Socioeconomic Data and Applications Centre (SEDAC), Columbia University. Available at http://sedac.ciesin.columbia.edu/gpw (last accessed 05-03-2009).

Gregory, J.M., Oerlemans, J., 1998, Simulated future sea-level rise due to glacier melt based on regionally and seasonally resolved temperature changes. Nature 391, 474-476.

Gregory, J.M., Huybrechts, P., 2006. Ice-sheet contribution to future sea-level change. Phil. Trans. R. Soc. A, 364, 1709-1731.

Gross, R., 2007. Earth rotation variations - long period. In: Herring, T.A. (ed.) Treatise on Geophysics, Oxford, Elsevier, 3, 239-294.

Hagedoorn, J.M., Wold, D., Martinec, Z., 2007. An Estimate of Global Mean Sea-level Rise Inferred from Tide-gauge Measurements Using Glacial-isostatic Models Consistent with the Relative Sea-Level Record. Pure and Applied Geophys 164, 791-818.

Heiskanen, W.A., Moritz, H. 1967. Physical Geodesy. Freeman, San Francisco.

Houghton, J.T., 2004. Global warming – The complete briefing. Cambridge University Press, Cambridge.

Huybrechts, P., de Wolde, J., 1999. The dynamic response of the Greenland and Antarctic ice sheets to multiple-century climatic warming. J. Climate 12, 2169-2188.

Huybrechts, P., Steinhage, D., Wilhelms, F., Bamber, J., 2000. Balance velocities and measured properties of the Antarctic ice sheet from a new compilation of gridded data for modelling. *Ann. Glaciol.*, 30, 52-60.

Huybrechts, P., Gregory, J., Janssens, I., Wild, M., 2004. Modelling Antarctic and Greenland volume changes during the 20th and 21st centuries forced by GCM time slice integrations. Global and Planetary Change, 42, 83-105.

Kuhn M., Seitz, K., 2005, Comparison of Newton’s integral in the space and frequency domains. In: Sansò, F. (Ed.), International Association of Geodesy Symposia 128: A Window on the Future of Geodesy. Springer, Berlin, Heidelberg, pp. 386-391.

Lambeck, K., Esat, T.M., Potter, E.-K., 2002. Links between climate and sea-level for the past three million years. Nature 419, 199-206.

Lambeck, K., Purcell, A., Johnston, P., Nakada, M., Yokoyama, Y., 2003. Water-load definition in the glacio-hydro-isostatic sea-level equation. Quaternary Sci Res 22, 309-318.

Lemoine, F.G., Kenyon, S.C., Factor, J.K., Trimmer, R.G., Pavlis, N.K., Chinn, D.S., Cox, C.M., Klosko, S.M., Luthcke, S.B., Torrence, M.H., Wang, Y.M., Williamson, R.G., Pavlis, E.C., Rapp, R.H., Olson, T.R., 1998. The development of the NASA GSFC and National Imaginary and Mapping Agency (NIMA) Geopotential Model EGM96, Rep. NASA/TP-1998-206861. NASA, Maryland.

Luthcke, S.B., Zwally, H.J., Abdalati, W., Rowlands, D.D., Ray, R.D., Nerem, R.S., Lemoine, F.G., McCarthy, J.J., Chinn, D.S., 2006. Recent Greenland Ice Mass Loss by Drainage System from Satellite Gravity Observations. Science 314, 1286, doi:10.1126/science.1130776.

Lythe, M.B., Vaughan, D.G., BEDMAP Consortium, 2001. BEDMAP: A new ice thickness and subglacial topographic model of Antarctica. J. Geophys. Res. 106, 11,335-11,351.

Makarynskyy, O., Kuhn, M., Featherstone, W. E., 2007. Long-term sea-level projections with two versions of a global climate model of intermediate complexity and the corresponding changes in the Earth's gravity field. Computers & Geosci 33 (8), 1036-1051, doi: 10.1016/j.cageo.2006.11.003.

Milne, G.A., Mitrovica, J.X., 1998. Postglacial sea-level on a rotating Earth. Geophys. J. Int. 133, 1-19.

Milne, G.A., Mitrovica, J.X., Davis, J.L., 1999. Near-field hydro-isostasy: the implementation of a revised sea-level equation. Geophys. J. Int., 139: 464-482.

Mitrovica, J.X., 2003. Recent controversies in predicting post-glacial sea-level change. Quaternary Sci Rev 22, 127-133.

Mitrovica, J.X., Milne, G.A., 2003. On post-glacial sea-level: I. General theory. Geophys. J. Int. 154, 253-267.

Mitrovica, J.X., Tamisiea, M.E., Davis, J.L., Milne, G.A., 2001. Recent mass balance of polar ice sheets inferred from patterns of global sea-level change. Nature 409, 1026-1029.

Mitrovica, J.X., Wahr, J., Matsuyama, I., Paulson, A., 2005. The rotational stability of an ice-age earth. Geophys. J. Int., 161, 491-506.

Mitrovica, J.X., Gomez, N., Clark, P.U., 2009. The Sea-Level Fingerprint of West Antarctic Collapse. Science, 323, 753.

Nakiboglu, S.M., Lambeck, K., 1991. Secular sea-level change. In: Sabadini, R., Lambeck, K., Boschi, E., (Eds.), Glacial Isostasy, Sea-Level and Mantleel Rheology. Kluwer Academic, Dordrecht, Netherlands, pp. 237-258.

Nerem, R.S., Mitchum, G.T., 2001. Observations of sea-level change from satellite altimetry. In: Douglas, B.C., Kearney, M.S., Leatherman, S.P. (Eds.), Sea-level Rise, History and Consequences. Academic Press, London, pp. 121-163.

Nicholls, R.J., 2002. Analysis of global impacts of sea-level rise: a case study of flooding. Phys Chem Earth 27, 1455-1466.

Oki, T., Kanae, S., 2006. Global Hydrological Cycles and World Water Resources. Science 313, 1068-1072.

Oppenheimer, M., 1998. Global warming and the stability of the West Antarctic Ice Sheet. Nature 404, 325-331.

Peltier, W.R., 2001. Global Glacial Isostatic Adjustment and Modern Instrumental Records of Relative Sea-level History. In: Douglas, B.C., Kearney, M.S., Leatherman, S.P. (Eds.), Sea-level Rise, History and Consequences. Academic Press, London, pp. 65-95.

Pilkey, O.H., Cooper, J.A.G., 2004. Society and Sea-level Rise. Science, 303, 11781-1782.

Ramillen G., 2002. Gravity/magnetic potential of uneven shell topography. J Geod. 76, 139-149.

Raper, S.C.B., Braithwaite, R.J., 2006. Low sea-level rise projections from mountain glaciers and icecaps under global warming. Science, 439, 311-313.

Ridley, J.K., Huybrechts, P., Gregory, J.M., Lowe, J.A., 2005. Elimination of the Greenland Ice Sheet in a High CO_2 Climate. Journal of Climate, 18, 3409-3427.

Rignot E., Thomas, R.H., 2002. Mass Balance of Polar Ice Sheets. Science, 297, 1502-1506.

Roedelsperger, S., Kuhn, M., Makarynskyy, O., Gerstenecker, C., 2008. Steric sea-level channge and its impact on the gravity field caused by Global Climate Change. Pure and Applied Geophys 165(6): 1131-1151.

Rowley, R.J., Kostelnick, J.C., Braaten, D., Li, X., Meisel, J., 2007. Risk of Rising Sea-level to Population and Land Area. EOS 88, 105-107.

Slolomon, S., Qin, D., Manning, M., Alley, R.B., Berntsen, T., Bindoff, N.L., Chen, Z., Chidthaisong, A., Gregory, J.M., Hegerl, G.C., Heimann, M., Hewitson, B., Hoskins, B.J., Joos, F., Jouzel, J., Kattsov, V., Lohmann, U., Matsuno, T., Molina, M., Nicholls, N., Overpeck, J., Raga, G., Ramaswamy, V., Ren, J., Rusticucci, M., Somerville, R., Stocker, T.F., Whetton, P., Wood, R.A., Wratt, D., 2007. Technical Summary. In: Slolomon, S., Qin, D., Manning, M., Chen, Z., Marquis, M., Averyt, K.B., Tignor, M., Miller, H.L. (Eds.), Climate Change 2007: The Physical Science Basis. Contribution of Working Group I to the Fourth Assessment Report of the Intergovernmental Panel on Climate Change. Cambridge University Press, Cambridge, United Kingdom and New York, USA, pp. 19-91.

Tamisiea, M.E., Mitrovica, J.X., Milne, G.A., Davis, J.L., 2001. Global geoid and sea-level changes due to present-day ice mass fluctuations. J. Geophys. Res. 106, 30,849-30,863.

Velicogna, I., Wahr, J., 2006. Measurements of Time-Variable Gravity Show Mass Loss in Antarctica. Science 311, 1754-1756.

Williams Jr., R.S., Ferrigno, J.G., 1999. Satellite image atlas of glaciers of the world, Prof. Pap. 1386-A. U.S. Geol. Survey, Reston, chap. A.

Woodward, R.S., 1888. On the form and position of mean sea-level. U.S. Geol. Survey Bull. 48, 87-170.

Woodworth, P.L., Player, R., 2003. The Permanent Service for Mean Sea-level: An update to the 21st century. J. Coastal Res. 19, 287-295.

Zhang, K., Douglas, B.C., Leatherman, S.P., 2004. Global Warming and Coastal Erosion. Climatic Change, 64, 41-58.

Fig. 1. Illustration of the physical principles behind the sea-level equation provided by eq. (1). The upper Panel A shows the current situation with huge ice sheets over the Polar Regions and the lower Panel B represents the situation after all ice masses have been melted.

Fig. 2. Global distribution of sea-level change due to a complete melt of the Greenland ice sheet together with all glaciers in the Northern Hemisphere (top) and a detailed view of the Arctic region (bottom). The maximum sea-level change (rise) is + 9.4 m (at 175.6ºE, 60.0ºS) and the minimum (fall) is – 24.4 m (at 51.5ºW, 70.9ºN) with a global average (eustatic) sea-level change of 6.8 m.

Fig. 3. Global distribution of sea-level change due to a complete melt of the Antarctic ice sheet together with all glaciers in the Southern Hemisphere (top) and a detailed view on the Antarctic region (bottom). The maximum sea-level change (rise) is + 72.1 m (at 148.5ºW, 80.6ºN) and the minimum (fall) is – 36.3 m (at 69.0ºE, 72.5ºS) with a global average (eustatic) sea-level change of 56.7 m.

Fig. 4. Global distribution of sea-level change due to a complete melt of all land based ice masses (top) and a detailed view of the Arctic region (bottom-left) and Antarctic region (bottom-right). The maximum sea-level change (rise) is + 78.5 m (at 162.4ºW, 46.2ºN) and the minimum (fall) is – 27.3 m (at 69.1ºE, 72.5ºS) with a global average (eustatic) sea-level change of 63.6 m.

Fig. 5. Global change in land-ocean distribution due to a complete [catastrophic] melt of all land-based ice masses. The flooded regions (indicated in red) are the result of comparing the

spatially variable sea-level change in Figure 3 with the topographic heights and ocean depths from JGP95E (given in metres). Over ice covered areas the elevation of the bedrock (set to 0 m if bedrock is below current mean sea-level) has been taken.

Table 1. Ice volumes given by JGP95E (Lemoine et al., 1998, chapter 2) and their eustatic sea-level equivalents. Estimates are presented for all ice masses (first two estimates) and ice masses that are located above current sea-level (last two estimates).

Component	Total ice masses		Ice masses above current mean sea-level	
	Volume $[10^6\ km^3]$	Sea-level equivalent [m]	Volume $[10^6\ km^3]$	Sea-level equivalent [m]
Antarctica	25.6	64.9	22.4	56.7
Greenland	2.67	6.8	2.64	6.8
Glaciers	0.036	0.09	0.033	0.09
Total	**28.4**	**71.8**	**25.1**	**63.6**

Table 2. Change in the Earth's gravitational oblateness (J_2), length of day (LOD) and centre of mass expressed in the geocentric coordinate differences ΔX, ΔY and ΔZ based on the three different melting scenarios.

Melting scenario	Change in $J_2 \times 10^{-6}$ [-]	Change in LOD [sec]	Change in the Earth's centre of mass		
			ΔX [m]	ΔY [m]	ΔZ [m]
A: Greenland ice sheet and glaciers in the Northern Hemisphere	+0.26	+0.04	-0.9	+0.4	-3.1
B: Antarctic ice sheet and glaciers in the Southern Hemisphere	+2.36	+0.41	-2.6	-4.5	+21.2
C: Complete melt of all land-based ice masses	+2.62	+0.46	-3.5	-4.1	+ 18.1

Table 3. Biases (relative errors) in eustatic sea-level estimates due to insufficient spatial sampling of the global oceans by tide-gauge stations and satellite altimetry (here, the TOPEX/Poseidon mission). Positive/negative values indicate an overestimation/underestimation with respect to the 63.6 m eustatic (global average) sea-level change estimate as given by all grounded ice masses above current MSL contained in JGP95E (cf. Table 1).

Melting scenario	27 tide-gauge stations selected by Douglas et al. (2001) [%]	1957 tide-gauge stations provided by PSMSL (Woodworth and Player , 2003) [%]	TOPEX/Poseidon (limited to ± 66° in latitude, e.g. Fu and Cazenave 2001) [%]
A: Greenland ice sheet and glaciers in the Northern Hemisphere	-11.2	-8.4	+2.9
B: Antarctic ice sheet and glaciers in the Southern Hemisphere	+14.1	+11.6	+0.7
C: Complete melt of all land-based ice masses	+11.4	+9.5	+4.2

Table 4. Extent of flooding for our three scenarios characterised by the relative change in land and ocean areas, the adjustment of the global average sea-level according the water involved in flooding of low-lying areas and the amount of current world population affected.

Melting Scenario	Relative change in land area [%]	Relative change in ocean area [%]	Relative adjustment of global average sea-level change [%]	Amount of world population affected [%]
A: Greenland ice sheet and glaciers in the Northern Hemisphere	-1.3	+0.5	-0.4	4.5
B: Antarctic ice sheet and glaciers in the Southern Hemisphere	-8.8	+3.6	-3.0	27.1
C: Complete melt of all land-based ice masses	-10.0	+4.1	-3.2	29.1

[Figure 1]

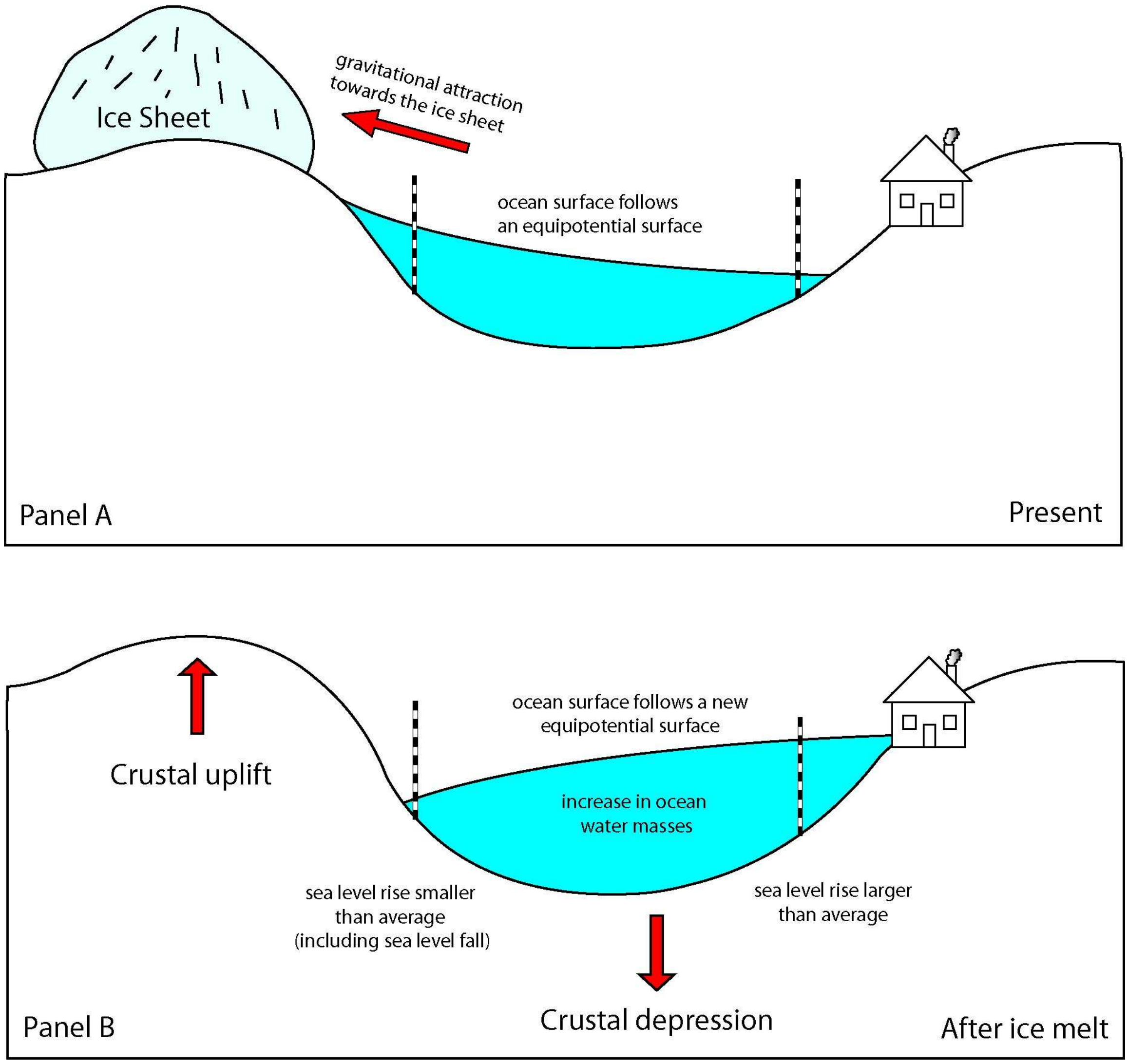
Ice Sheet
gravitational attraction towards the ice sheet
ocean surface follows an equipotential surface
Panel A
Present
Crustal uplift
ocean surface follows a new equipotential surface
increase in ocean water masses
sea level rise smaller than average (including sea level fall)
sea level rise larger than average
Crustal depression
Panel B
After ice melt

[Figure 2]

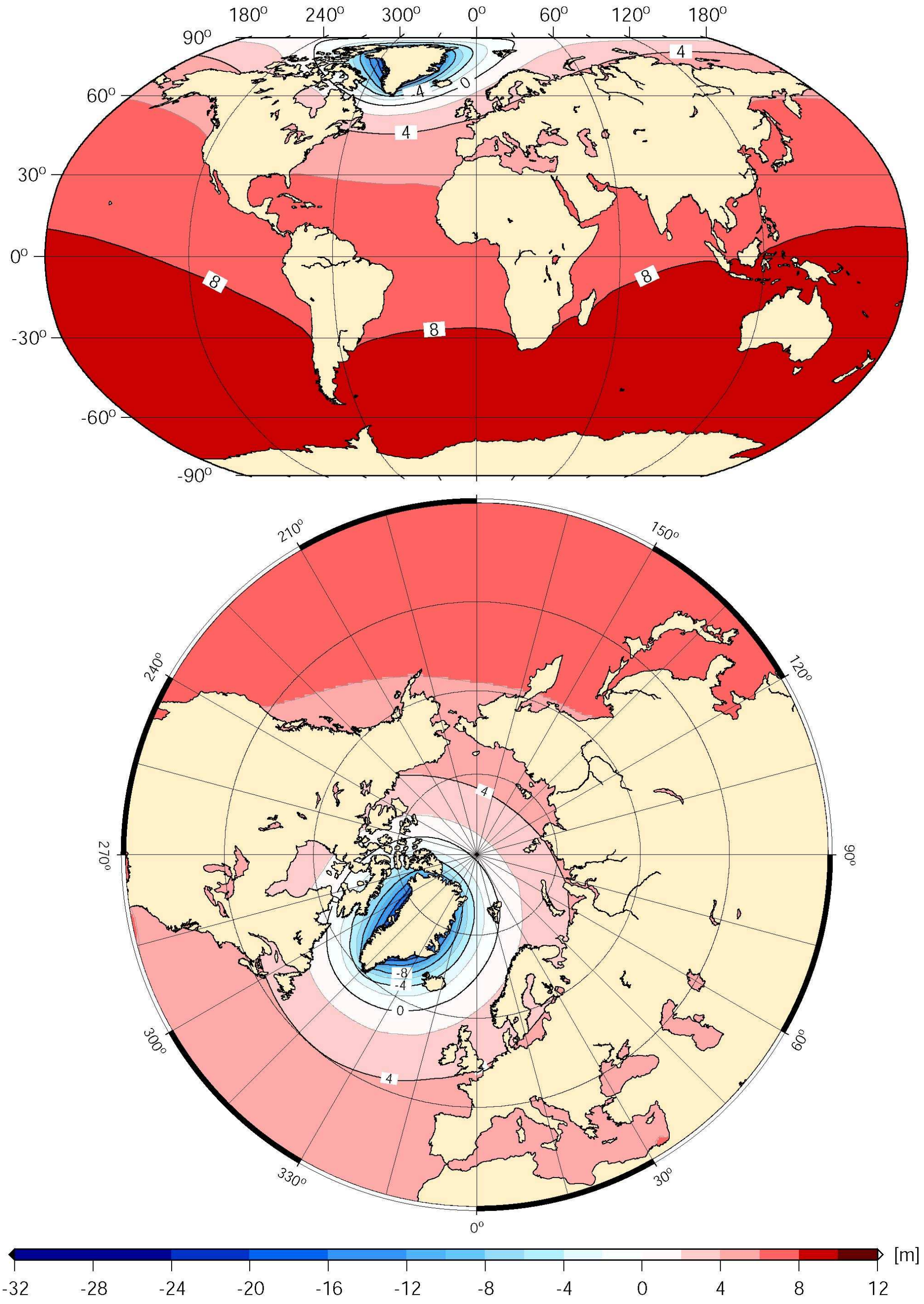

180°
240°
300°
0°
60°
120°
180°
90°
60°
30°
0°
-30°
-60°
-90°
4
0
-4
4
8
8
8
210°
150°
240°
120°
270°
90°
300°
60°
330°
30°
0°
4
-8
-4
0
4
-32
-28
-24
-20
-16
-12
-8
-4
0
4
8
12
[m]

674 **[Figure 3]**

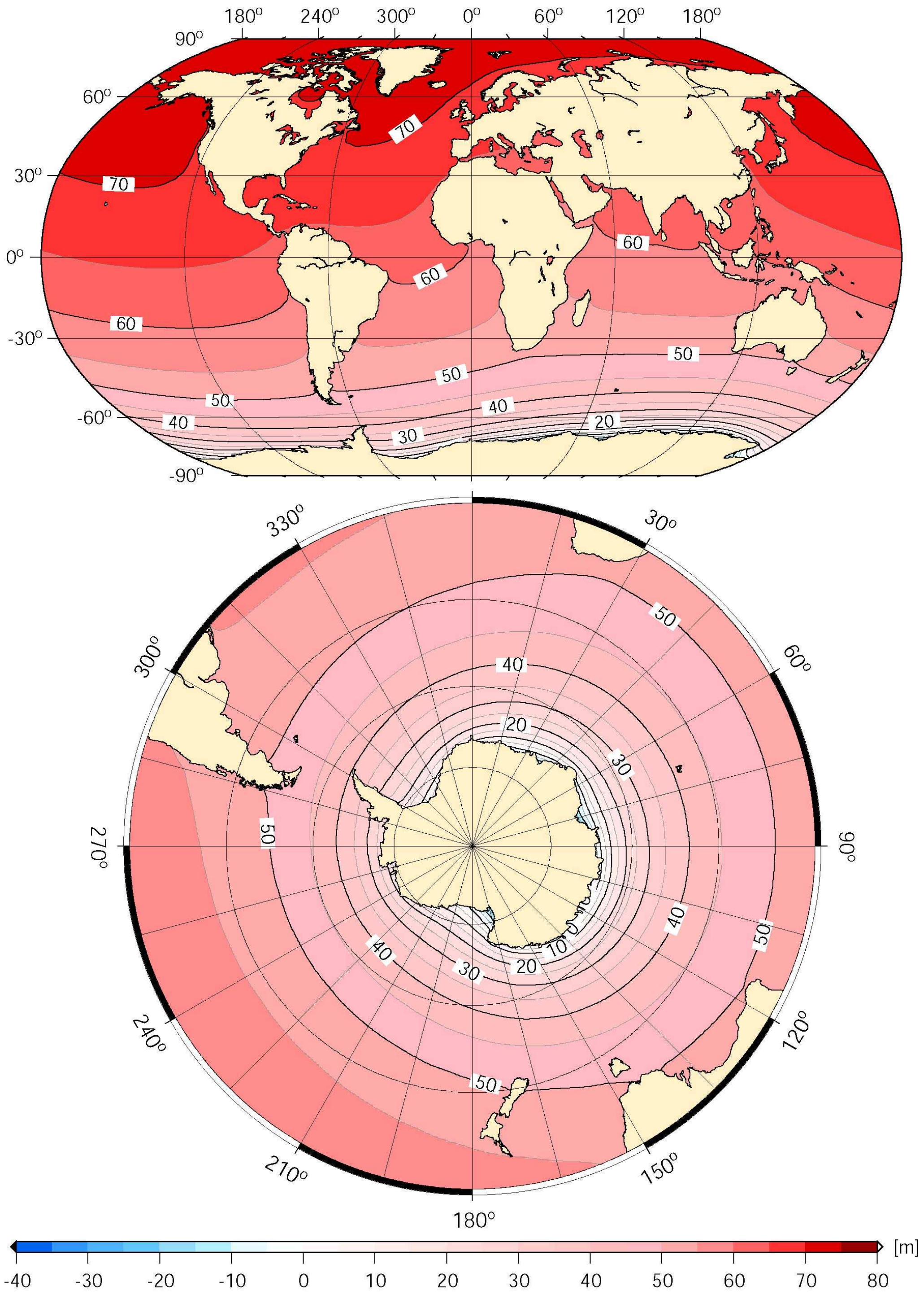

675

676 **[Figure 4]**

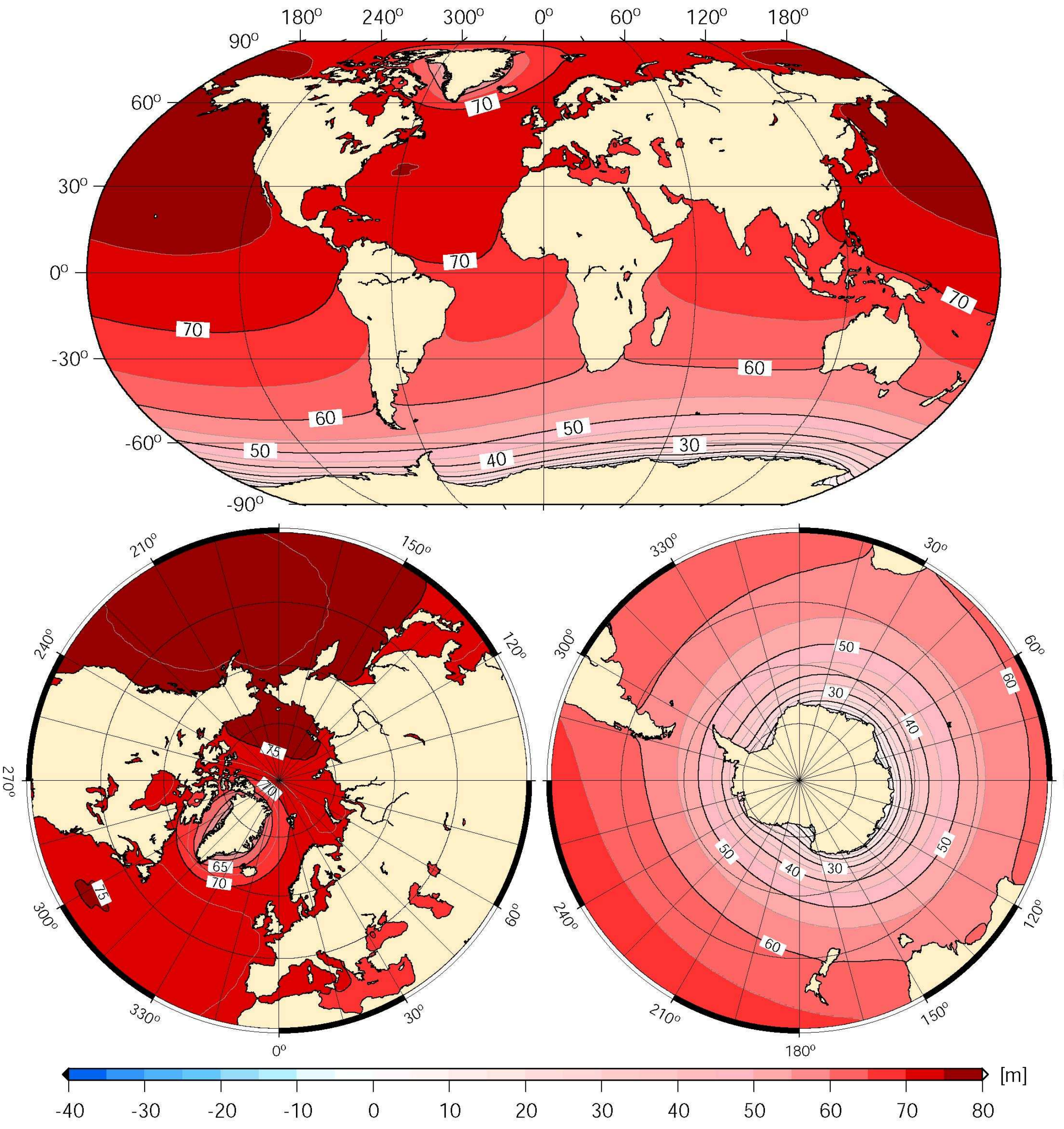

677

[Figure 5]

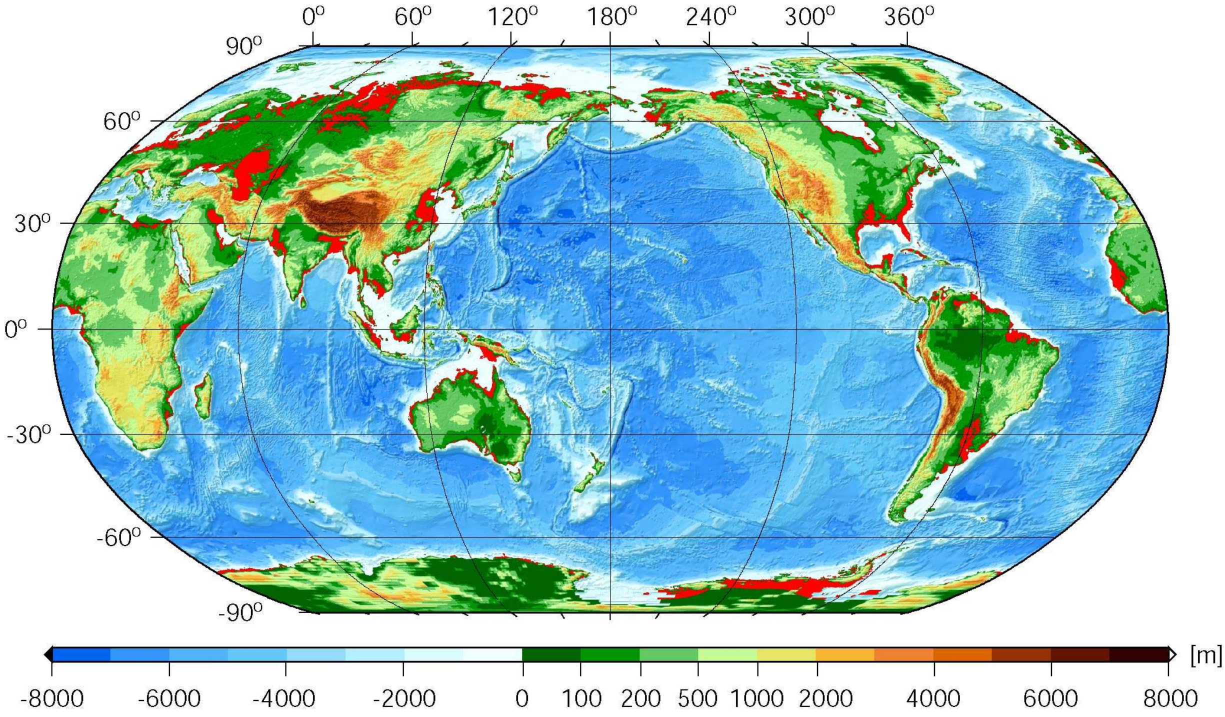
0°
60°
120°
180°
240°
300°
360°
90°
60°
30°
0°
-30°
-60°
-90°
[m]
-8000
-6000
-4000
-2000
0
100
200
500
1000
2000
4000
6000
8000